# Population size fluctuations can drive multitrait diversification in marine diatoms

Jana Hinners[a,b], Phoebe A. Argyle[c], Nathan G. Walworth[d], Martina A. Doblin[c,e], Naomi M. Levine[d], Sinéad Collins[b,*]

[a]Helmholtz-Zentrum Hereon, Max-Planck-Straße 1, 21502 Geesthacht, Germany
[b]Institute of Ecology and Evolution, University of Edinburgh, Charlotte Auerbach Road, Edinburgh, EH9 3FL United Kingdom
[c]Climate Change Cluster, University of Technology Sydney, Sydney, New South Wales 2007, Australia
[d]Department of Biological Sciences, University of Southern California, Los Angeles, CA 91011, Unites States of America
[e]Sydney Institute of Marine Science, Mosman, New South Wales 2088, Australia

*Corresponding author: Sinead Collins
**Email:** s.collins@ed.ac.uk

**Author Contributions:** S.C., N.L. and M.D. designed research; S.C. and J.H. planned experiments; J.H.performed laboratory work and carried out data analysis; all authors contributed to data analysis and writing the paper.

**Competing Interest Statement:** The authors declare to have no competing interests.

**Keywords:** phytoplankton, bottleneck experiment, experimental evolution, trait-based approach, principal component analysis

## Abstract

Phytoplankton are photosynthetic marine microbes that play key roles in food webs, nutrient cycles, and climate regulation. These roles are determined by a correlated set of phytoplankton functional traits, including cell size, chlorophyll content, and cellular composition. Correlations between functional traits are often considered as stable pairwise relationships. However, both pairwise and higher order correlations between traits exist and can evolve. We used a laboratory experiment with six genotypes of Thalassiosirid diatom to explore how trait values and higher-order trait correlations constrain pattens of trait diversification following common occurrences – reductions in population size, and mild warming. We analysed the simultaneous evolution of nine functional traits and their correlations on a trait-scape that collapses multitrait variation onto a reduced set of axes. We found that the trait-scape was relatively stable over time, in that the trait-scape defined by the ancestral populations also captured the variation in evolved populations. This reveals patterns and constraints on multitrait evolution in the genus. Population bottlenecks - transient but severe reductions in population size - facilitated infrequent shifts in trait-scape during evolution, while population bottlenecks combined with warming allowed more frequent shifts. Movement of evolving populations on the trait-scape was associated with both changes in trait values and trait correlations. Our study highlights that first, transient reductions in population size can drive phenotypic diversification in diatoms. Dramatic reductions in population size may be relevant for natural populations due to drops in population size between phytoplankton blooms, or during migration between currents. Second, higher order trait correlations matter. While few obvious patterns exist in the evolution of individual trait values across our experiment, the trait-scape defined by multiple traits and their correlations reveals consistent patterns of phenotypic evolution.

## Significance Statement

Diatoms are a highly diverse group of phytoplankton that play key roles in ocean ecology and biogeochemistry. They do this through many interrelated functional traits (eg. cell size, elemental composition, chlorophyll content). Little is known about how correlations beyond pairwise tradeoffs affect multitrait change in diatoms, or about the stability of trait correlations in the face of common demographic or environmental shifts. We used experimental evolution that incorporated population bottlenecks, consistent with bloom-and-bust growth or advection between ocean currents, to assess patterns of multitrait evolution in the diatom genus *Thalassiosira*. Population bottlenecks enabled rapid shifts in both trait values and trait correlations even in a stable environment, and these shifts were more frequent under moderate warming, however constraints on multitrait evolution were evident. This indicates that multitrait diversification is driven by demographic shifts (a common feature of phytoplankton growth strategies) and modest environmental change. This highlights the importance of higher-order trait correlations in phytoplankton evolution, and impacts the way related functional traits in phytoplankton are conceptualized and modeled.

## Introduction

Phytoplankton functional traits such as cell size, elemental composition, and population growth rates are crucial to the roles that phytoplankton play in ocean ecology and biogeochemical cycling. Functional traits are highly diverse across phytoplankton, allowing them to thrive in all aquatic environments. This diversity is shaped both by natural selection and by patterns of migration determined by physical forces such as ocean currents ([1]). Natural selection can act on pre-existing trait variation between phytoplankton lineages, species, or functional groups ([2,3]), but can also act on novel trait variation generated by genetic mutation or heritable epigenetic effects ([4]). This allows for potentially rapid evolution of multiple functional traits within phytoplankton lineages ([5]). Modeling, predicting, and explaining functional trait evolution requires defining how patterns of trait variation in viable populations can change – this variation is what natural selection subsequently acts on. Understanding constraints on how interrelated functional traits can change simultaneously is vital for projections of trait changes in phytoplankton, and subsequent effects on ecology and biogeochemistry.

One key driver of trait change is the strength of natural selection, which depends crucially on population size. In some marine microbes, such as diatoms, extreme fluctuations in population size occur both during bloom and bust growth, and as a result of the physical forces in ocean currents. Phytoplankton are at the mercy of oceanographic currents, which transport them relatively rapidly across different ecoregions ([6,7]). While environmental fluctuations within currents can affect trait evolution in large phytoplankton populations ([6,8]), the effect of the demographic fluctuations that go along with life in this dynamic ocean environment have yet to be incorporated into our understanding of phytoplankton diversity. However, there is every indication that fluctuations in population size are important to phytoplankton trait evolution. Population bottlenecks and subsequent founder events can affect diversity patterns ([9]) and phenotype evolution. In particular, bottlenecks can result in high local diversity, but low effective population sizes ([9,10]). There are growing observations of patterns of diversity in marine microbes that are consistent with population bottlenecks playing an important role in these systems. For example, high-resolution simulations demonstrated that common phenomena in microbial environments such as swift current speeds, fast dispersal, and increased environmental variability favored patterns of local diversity ([11]), indicating that bottlenecks may be a common phenomenon. Founder effects have been detected in fjord and limnic ecosystems ([12,13]), and may be enhanced by propagule banks buffering against new immigrants ([13]). Recent analyses of effective population sizes of one of the most abundant primary producers in oceans, *Prochlorococcus*

*marinus,* were orders of magnitude lower than previously predicted ([14]), suggesting that founder effects may play an important role in shaping population genetic structure, even in abundant marine microbes. Additionally, microcosm experiments with the diatom *Skeletonema marinoi* revealed that founder effects can be important even if immigrants make up a high proportion of local populations ([15]) .

Phytoplankton diversity is often framed in terms of variation in phytoplankton functional traits, such as cell size ([16,17]). Functional traits of diatoms are well studied, and usually considered as pairwise correlations, often involving fundamental tradeoffs between traits, such as cell size and nutrient uptake affinity ([18,19]). Based on this, trait-based models of diatoms and other phytoplankton often use the simplifying assumption that fitness is determined by a single master trait (e.g. size), and that all other traits are linked through a fixed correlation with the master trait ([16]). This therefore assumes that trait correlations are maintained during evolution, and that pairwise correlations are sufficient to describe constraints on complex phenotypes. However, multitrait relationships that extend beyond pairwise correlations can constrain phenotypic change on both plastic ([20,21]) and evolutionary ([22]) timescales. In addition, adaptive outcomes are consistent with these correlations shifting during adaptation ([22]). These multitrait relationships can be identified through statistical techniques such as principal component analyses (PCA), which can define the “trait-scape” possible for phytoplankton phenotypes ([20]) in one or more environments. The trait-scape collapses multitrait variation onto a reduced set of axes, which allows us to study variation in multitrait phenotypes rather than in single traits. In contrast to master trait approaches, trait-scapes can be used to study shifts in trait correlations as well as in trait values.

Here, we use diversification driven by population bottlenecks to explore the potential for evolutionary change in functional traits that affect the ecosystem and biogeochemical function of temperate diatoms. The experiment used six genetically and phenotypically distinct strains, in replicate. For clarity, we refer to each starting genotype as a strain and to each evolving replicate population that is related by descent as a lineage. See Fig. 5 for a schematic of the experiment. Briefly, we used repeated population bottlenecks to increase genetic and phenotypic divergence between replicate populations. During bottlenecks, relaxed stabilizing selection allows sub-optimal but viable multitrait phenotypes to emerge (reduced selection – RS – phase of experiment) because chance, rather than natural selection, plays a dominant role in which cells survive. We then observed how natural selection acts on this trait variation by evolving the lineages as large populations. Natural selection is effective in large populations, so fitter multitrait phenotypes increase in frequency within each population (full selection – FS – phase of experiment). The experiment ended when population growth rates stabilized, indicating that FS populations were on or near local phenotypic optima, and that variation underlying large differences in fitness that was generated during the RS phase had been used by natural selection. It does not preclude that further evolution, especially with a supply of novel mutations, would allow fitness to eventually increase further ([23]); this is true of all microbial evolution experiments. We consider whether populations return to their ancestral multitrait phenotype over this timescale, move to an area of the trait-scape occupied by a different genotype, thus connecting two peaks, or discover a novel peak in the trait-scape (see Box 1). This provides insight into patterns of multitrait variation in diatoms, and into constraints on multitrait diversification under demographic fluctuations.

**Box 1: Trait-scapes and movement in trait-scapes**

Trait-scapes collapse multitrait variation onto a reduced set of (principle component) axes. While they resemble fitness landscapes and provide insight into evolutionary patterns and constraints for functional traits, trait-scapes differ from fitness landscapes in three key respects. First, trait-scapes do not need to include fitness as one of the axes, whereas fitness landscapes do. This follows from the starting point that any strains used to generate the trait-scape are “fit enough” to persist in the environment that they were sampled from. Because of this, we refer to locations occupied by ancestors and populations under full selection as “peaks” in the trait-scape, although the height of these peaks is not defined. Second, because trait-scape axes are combinations of traits rather than single traits, single locations in the trait-scape space can contain more than one multitrait phenotype ([22]). In the context of a trait-scape, these are called cryptic phenotypes. In contrast, each point on a fitness landscape represents a single genotype or phenotype. Finally, because fitness depends on the environment, fitness landscapes are necessarily environment-specific. However, because trait-scapes need not include fitness as an axis, phenotypes from multiple environments can be compared on a single trait-scape to reveal fundamental relationships in multitrait phenotypes that hold across environments.

Movement in trait-scapes can be the result of changes in trait values, trait correlations, or both. Figure B1 shows possible types of movement in the trait-scape. Reduced selection will result in populations moving from their ancestral peak in the trait-scape (grey) to, on average, lower-fitness locations (orange). Movements in the trait-scape during the full selection phase are shown in blue. If trait values and correlations are strongly constrained, populations may recover trait values similar to their ancestor and be on "isolated" peaks. Alternatively, if trait values and correlations are less constrained, evolving populations may move to a new peak. If this new peak has a similar trait value combination to another ancestral population, the ancestral peaks are "connected" via a fitness valley that can be traversed. Otherwise, populations may move to a previously unoccupied location in the trait-scape under full selection, finding a "novel" peak. If only trait values evolve, movement in the trait scape will be constrained by this and most peaks will be isolated. If trait correlations also evolve, all three types of movements should occur.

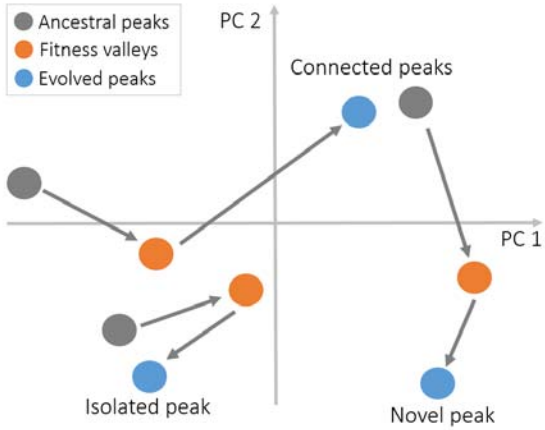


**Figure B1.** Schematic of the three possible movements in the trait-scape.

## Results

***Effectiveness of population bottlenecks and fitness recovery.*** The goal of our study was to examine patterns of change in multitrait phenotypes in diatoms. We assume that our ancestral populations were well adapted to the culture conditions and thus sat on relatively high fitness peaks within the trait-scape. Our rationale for this assumption is that the ancestral strains had high enough fitness to be sampled and survive isolation, were all from culture collections, and had been grown in similar laboratory conditions for five months prior to the start of the experiment. The population bottlenecks resulted in lower fitness with an average reduction in growth rate to 17-65% compared to ancestral rates (Fig. S3), as well as with different multitrait phenotypes compared to their ancestors (Fig. S6). Though growth rate may not be a complete description of fitness, large reductions in population growth rate in batch culture have a negative impact on overall fitness. This reduction in growth during the bottleneck phase of the experiment further supports the assumption that the ancestral populations were relatively well-adapted to the laboratory environment to start with. Following population bottlenecks, fitness recovery was effective, and full selection populations under control (FSC) and high temperature conditions (FSH) evolved growth rates that stabilized at similar values to control populations propagated in the same environment as large populations (Fig. S4).

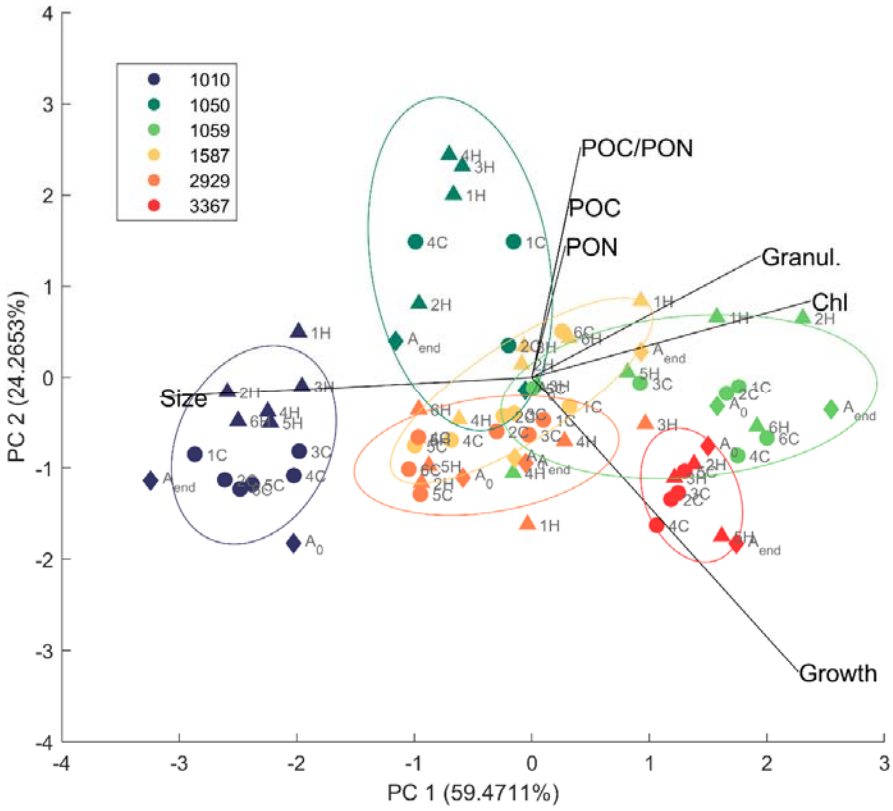


**Figure 1.** The trait-scape based on the principal component analysis of all ancestral ($A_0$ and $A_{end}$) and evolved (FSC and FSH) populations. Trait values were obtained under control conditions. Ancestors, FSC and FSH evolved populations are visualized together, colour-coded by strain. Ancestors are marked with a diamond, FSC populations with a circle, and FSH populations with a triangle. Replicates from the reduced selection are indicated by numbers, $A_0$ and $A_{end}$ mark the ancestral populations measured at the beginning and end of the experiment. Circles represent 75% confidence intervals for each strain.

***The trait-scape.*** Previous work demonstrated that the ancestral multitrait *Thalassiosira* phenotypes could be studied using a reduced axis of variation trait-scape ([20,24]). Our

experiments allowed us to assess the structure of the *Thalassiosira* trait-scape, in particular evaluating the ruggedness of the trait-scape (*see Box 1*). To do this, we combined the ancestral and evolved populations into one principal component analysis (Fig. 1). The first two principal components of the trait-scape explain almost 85% of the variation in trait values of nine functional traits (population growth rate, cell size, cell complexity, chlorophyll a content, particulate organic carbon and nitrogen, lipid content, silicic acid uptake, intracellular reactive oxygen; see Methods). Interspecific variation across strains (indicated by different colors) was significantly larger than within strain variation over the course of the experiment ($F_{1,11338} = 1256$, $p<0.01$). Location in the trait-scape was strain-specific as in previous experiments using these ancestral strains ([20]). Most strains stayed on or returned to their ancestral peak after bottlenecking, suggesting that the trait-scape for the *Thalassiosira* genus is rugged, with well-separated fitness peaks surrounded by lower-fitness valleys. Overall, the trait-scape was evenly filled by the six strains, without large gaps that would indicate non-allowable trait value combinations within the space defined by the first two principal components. This result is consistent with previous experiments with these strains ([20]). Assessment of changes in single traits across the experiment and the movement of strains in the trait-scape including all reduced selection stages is provided in Fig. S6 and Fig. S7.

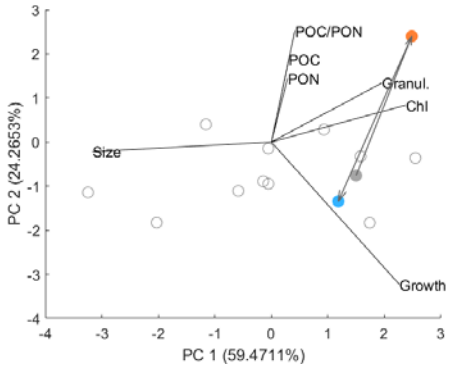


a) Isolated peak, 3367-2C

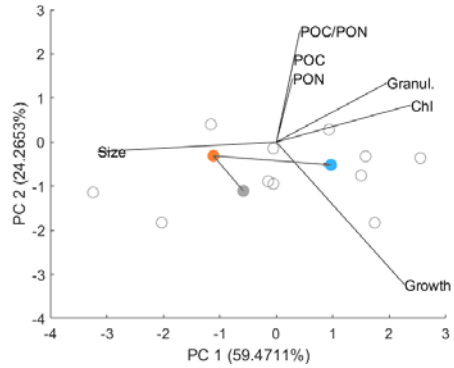


b) Connected peak, 2929-3H

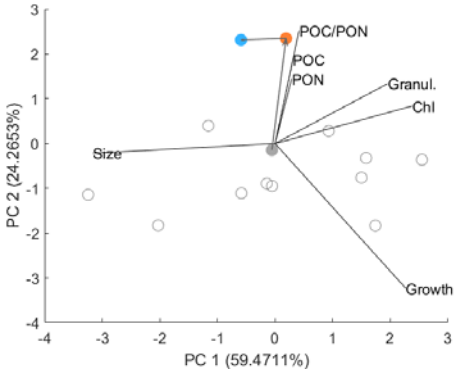


c) Novel peak, 1050-3H

| 1010 | 1050 | 1059 | 1587 | 2929 | 3367 |
|---|---|---|---|---|---|
| 1C | 1C | 1C | 1C | 1C - 1587 | 2C |
| 2C | 2C | 2C | 2C | 2C | 3C |
| 3C | 4C | 3C | 3C | 3C | 4C |
| 4C | | 4C | 4C | 4C | 5C |
| 5C | | 5C | 5C - 2929 | 5C | |
| 6C | | 6C | 6C | 6C | |
| 1H | 1H | 1H | 1H - 1059 | 1H | |
| 2H | 2H | 2H | 2H | 2H | 2H |
| 3H | 3H | 3H | 3H | 3H - 3367 | 3H |
| 4H | 4H | 4H | 4H | 4H - 1587 | 5H |
| 5H | | 5H | 5H - 2929 | 5H | |
| 6H | | 6H | 6H | 6H | |

Isolated peak
Connected peak
Novel peak

d) Categorization of all populations

**Figure 2.** Example movements of three populations (3367-2C, 2929-3H, and 1050-3H) in the trait-scape (a-c). The principal component analysis was performed based on trait data from ancestral, FSC and FSH populations; reduced-selection populations were projected into this trait-scape. Data from all ancestors ($A_0$ and $A_{end}$) are depicted in grey, unfilled circles. Arrows follow the movements from an ancestral population ($A_0$, grey filled circle) to its location after reduced selection (orange), and then to its location after full selection (blue). (d) Categorization of all populations into isolated, connected or novel peaks. In case of connected peaks, the connected strain is mentioned. Populations are sorted by strains, numbers represent reduced selection replicate identities, and letters indicate full selection conditions (C - control or H - high temperature).

***Changes in multitrait phenotypes.*** We used the movement of populations on the trait-scape to define patterns of change to multitrait phenotypes in two environments. In the first, FSC populations evolved in the ancestral environment, so that any phenotypic changes were not due to differences in environmentally-imposed selection between the ancestors and the FSC populations, but instead reflect changes in multitrait phenotypes that are the result of population bottlenecks only. In the second, FSH populations evolved in a warmed environment, where environmentally-imposed selection could also contribute to movement on the trait-scape. This allowed us to assess the impact of both rapid reductions in population size and of environmentally-imposed selection on multitrait phenotypes. We categorized movement in the trait-scape for each lineage as revealing either an isolated peak, a connected peak, or a novel peak (see Box 1, and "Analysis of trait-scape connectivity" in the Methods for more detail).

We observed all possible types of movement in the trait-scape (Fig. 2), with evidence for isolated, connected, and novel peaks (summarized in Fig. 2d). For both FSC and FSH populations (62 populations total), nine of the 62 populations (14.5%) moved to a novel peak in the trait-scape, six of the 62 (6.7%) moved to a connected peak and 47 of the 62 (75.8%) returned to their ancestral peak. Exploration of the trait-scape was limited, but not absent, when populations evolved under full selection in the ancestral environment. Of the 31 FSC populations, only one population found a novel peak, and only two populations moved to a connected peak. The two populations that found connected peaks were reciprocal – a single pair of peaks was connected on this landscape during our experiment (1587-2929). This indicates that first, the fitness landscape is reasonably well sampled in the ancestral environment and second, that it is possible for lineages to move on the trait-scape, and thus shift multitrait phenotypes, due to demographic perturbations alone.

Changes in multitrait phenotypes were more widespread when populations evolved in a different environment than their ancestor. Of the 31 FSH populations, four found connected peaks, evidencing three pairs of connected peaks on the trait-scape (1587-2929, 1587-1059, 3367-2929). In addition, eight FSH populations from two lineages located novel peaks, with strain 1010 often finding novel peaks. However, even when populations evolved in a different environment than their ancestors, the ancestral locations in the trait-scape captured a large proportion of the locations occupied by the FSH populations - only two of the six strains located novel peaks, though all six strains evolved novel multitrait phenotypes (i.e. different trait combinations). This is surprising, given that warming is known to drive adaptation in *Thalassiosira* ([25,26]). However, in this experiment, 19 out of 31 FSH populations returned to their ancestral location in the trait-scape. Our data therefore suggests that the outcome of adaptation to moderate warming, including shifts in multitrait phenotypes, varies between strains, and between replicate populations of the same strain, at least in cases where population bottlenecks occur.

***Patterns of multitrait evolution after population bottlenecks.*** Population bottlenecks transiently relax the efficacy of natural selection, and one particularly interesting consequence of this for trait-based approaches is the potential for rapid shifts in trait correlations as well as trait values. While most of the evolving populations returned to their ancestral locations in the trait-scape, novel trait combinations did sometimes occur following population bottlenecks.

Strains in locations categorized as isolated peaks in the trait-scape (1059 and 3367), showed no change from ancestral trait values when single traits are compared for the ancestral and FS populations of the same genotype (Fig. S7). Thus, even though many lineages evolved trait values different from their ancestors when selection was relaxed (RS phase) (Fig. S6, S7), most re-evolved ancestral trait values when selection was restored (FS phase). We were not able to measure all traits in the RS populations due to low growth and subsequent low biomass in these populations, so that changes in ROS, silica uptake and lipid content do not contribute to patterns on trait-scapes that include RS populations.

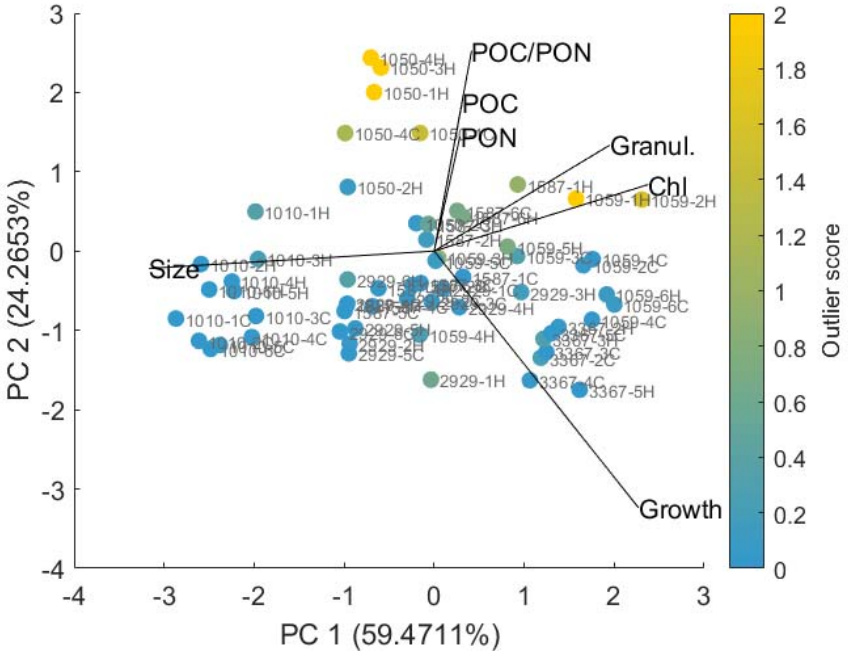


a) Trait-scape determined under control conditions

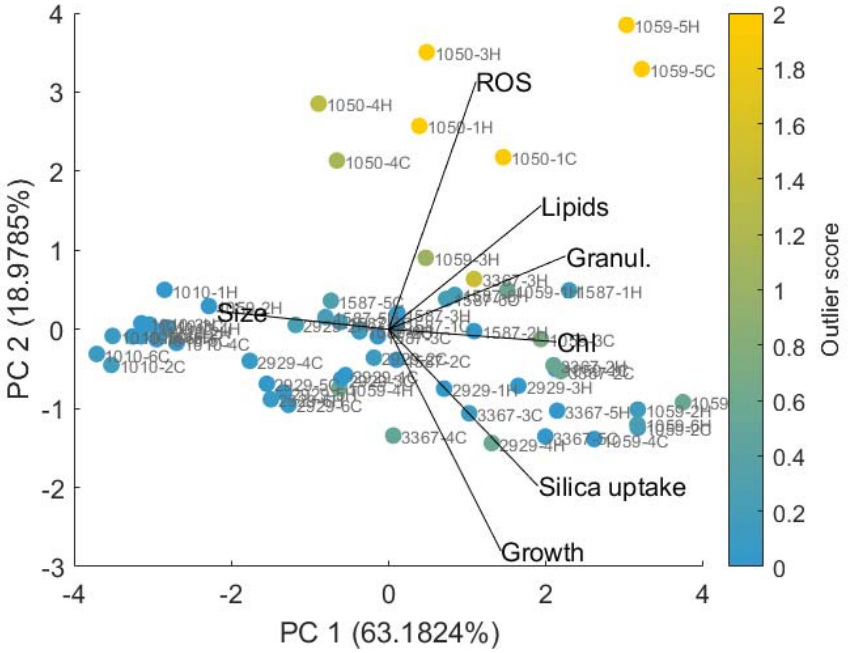


b) Trait-scape determined under high temperature conditions

**Figure 3.** The trait-scape of all FSC and FSH population measured under control (a) and high temperature (b) conditions, with outliers from ancestral trait correlations indicated by colour. Traits included in the principal component analysis differed between the two temperature conditions to include as many traits as possible, whilst maintaining comparability to the trait-scape that was calculated based on the available trait data of all ancestral, reduced selection and evolved lineages.

To categorize peaks using the full set of traits available in this study, we repeated the categorization above using only the ancestral and FS populations, so that the full set of traits

could be used (Fig. 3, 4, S9). We found large increases in ROS in lineages 1050-3H and 1050-4H, suggesting that our categorization of movement based on a trait-scape that includes the RS populations may underestimate novel peaks.

Interestingly, populations moving between connected peaks in the trait-scape did not evolve the same set of trait values as the ancestral strain originally on that peak (Fig. S11, S12). Instead, they developed multitrait phenotypes distinct from both their own ancestor and the ancestors or FS populations of other strains. This agrees with simulations of adaptation on trait-scapes ([22]) that predict the evolution of cryptic phenotypes, where more than one multitrait phenotype exists in a single location in trait-scape. This is exciting, because while novel multitrait phenotypes evolved, trait evolution was captured within the pre-existing trait-scape, and often involved moving to a location in the trait-scape occupied by a different strain.

**How do novel phenotypes evolve?** To learn whether novel multitrait phenotypes were associated with particular trait values, we quantified an outlier score for each FS population. This score identifies populations where the relationship between two traits has shifted substantially from the ancestral correlation (see ”Outlier analysis” in the Methods section). For FSC populations that evolved in the ancestral environment, we found that populations with high particulate organic carbon (POC) and nitrogen (PON) content, as well as high granularity and chlorophyll content depart most from ancestral trait correlations, whereas populations with large cell sizes and high growth rates depart least from ancestral trait correlations (Fig. 3(a)). FSH populations that evolved in the warmed environment showed a similar pattern, where populations with large cell sizes and high growth rates had lower outlier scores (Fig. 3(b)). In FSH populations, many populations with high outlier scores also had high reactive oxygen species (ROS) values, which suggests that large departures from ancestral trait correlations may be stressful for the cells (Fig. S9). This is consistent with previous work showing that ROS production is a common response to stressful environmental conditions ([27–29]).

To identify whether the evolution of novel phenotypes (high outlier scores) were associated with changes in specific trait correlations, we compared the mean residual values across strains for each pairwise trait correlation (Fig. 4(a)). Nine out of the ten most extreme outliers evolved under high temperature, suggesting that evolution in a new environment may favor changes in trait correlations (Fig. 4(b)). Across all outliers, the largest departure from ancestral trait correlations involved ROS, POC, PON, and lipid content (Fig. 4(a)), although more modest departures from ancestral correlations occurred in many other pairwise trait correlations. Taken together, this indicates that high outlier scores are typically associated with a substantial and directionally consistent (i.e. increase or decrease) change in a few key traits. This means that some traits are more likely to be associated with departures from ancestral trait correlations than are others. Second, it shows that some trait correlations evolve more readily than others, even without environmental change, suggesting that population bottlenecks can play an important role in transient trait correlation changes.

While evolution in trait correlations was relatively frequent across populations, the identity of the trait correlations that departed most from ancestral values were population-specific (Fig. 4(b)). 1050-3H, 1050-4H, 1059-3H and 1059-5H showed the most change from the ancestral correlations between ROS and other traits. 1050-1C and 1050-1H diverged most from ancestral correlations between lipid content and other traits, and 1059-1H and 1587-1H showed the most change from ancestral correlations between POC and PON content. Strains 1050 and 1059 had the greatest number of outlier populations, suggesting that these strains have more flexibility in trait correlations than the other strains in this study. Overall, the strongest departure from ancestral trait correlations was related to large shifts in correlation due to changes in a single trait (typically ROS).

Considering the relationship between growth and outlier scores provides information about the potential fitness effects of evolving new trait correlations, as population growth impacts fitness, especially during diatom blooms. We found that populations with large changes in trait correlations had reduced growth rates relative to their ancestral strain (Fig. S10), even though the stability of these growth rates indicated that those populations were on local optima at the end of the experiment. This indicates while trait correlations evolve readily after population bottlenecks, new trait correlations are likely to have a detrimental impact on fitness, so may be reversed if there is the opportunity for continued adaptation.

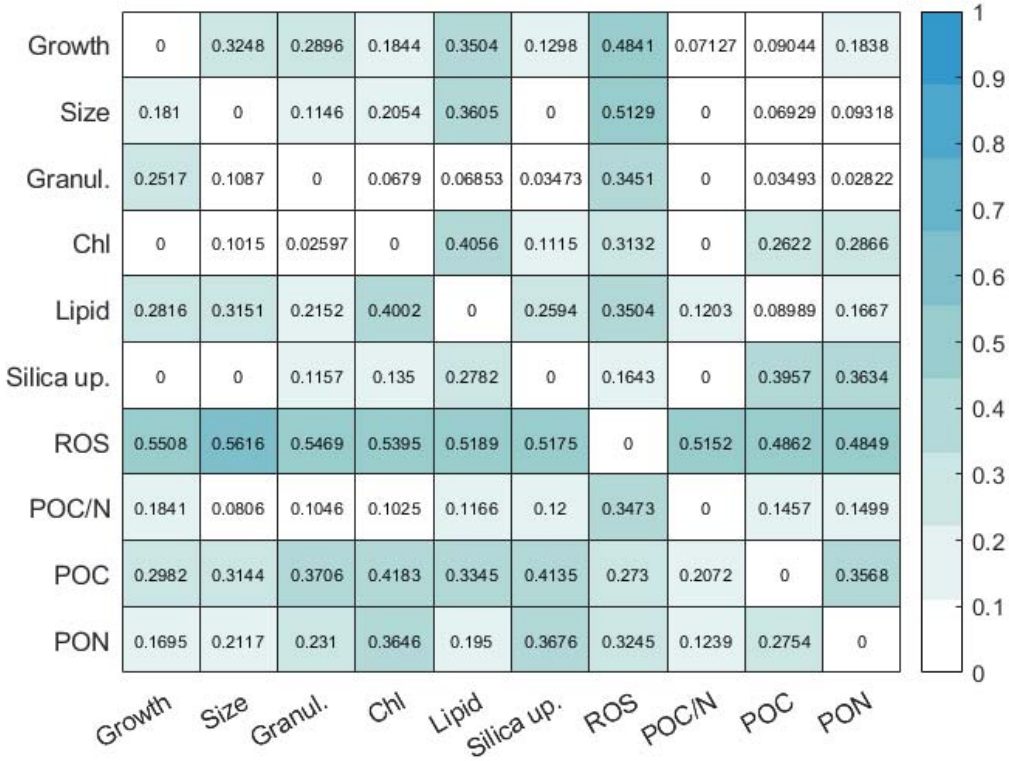


a) Average outlier score across all FSC and FSH populations for pairwise trait correlations

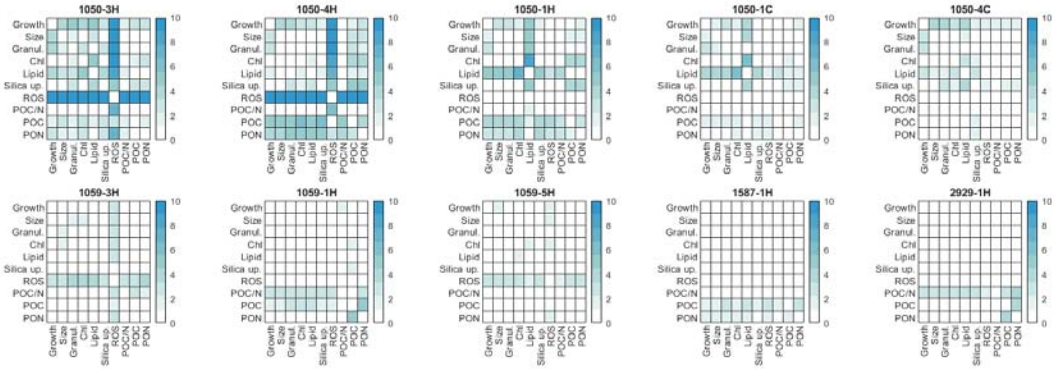


a) Individual outlier scores for all pairwise correlations for the 10 strongest outliers.

**Figure 4.** Outlier analysis for all pairwise trait correlations across strains (a) and for the 10 strongest outliers (b).

## Discussion

Observed variation in diatom phenotypes is generated by a variety of evolutionary forces including natural selection imposed both by the environment and by drastic fluctuations in population size (bottlenecks). The relationships between the many traits that define these phenotypes can be assessed using a trait-scape. Here, we used an evolution experiment where six phenotypically distinct lineages of the diatom genus *Thalassiosira* were allowed to "fall off" their ancestral multitrait phenotype peak using repeated population bottlenecks, and were subsequently re-evolved as large populations. We demonstrate that novel phenotypes emerged even in the absence of environmental selection and that the phenotypic shifts in the evolved populations could be studied using a the trait-scape defined by the ancestral populations. This suggests two fundamental insights. First, population bottlenecks can drive trait evolution in marine diatoms. This is likely to be important given the bloom and bust growth strategies of marine diatoms and the dynamic environments in which they live. Second, the trait-scape axes derived from the ancestral populations are relevant for understanding diatom evolution more generally because trait evolution is constrained to few fixed axes of variation, at least in the absence of substantial environmental change. This indicates that considering changes to multitrait phenotypes made up of numerous intertwined functional traits rather than as changes to single functional traits can reveal constraints on phenotypic evolution. Importantly, there are patterns to this trait variation, and they are discoverable using the trait-scape defined by the ancestors – evolution does not result needing in fundamentally new axes of variation.

In ecosystem modelling, phytoplankton multitrait phenotypes are often simplified by using a master trait, which determines the values of all other functional traits via fixed trait correlations ([16,17]). Here we demonstrate that, for our system, there is no master trait that can be used to understand how multitrait phenotypes evolved in the face of population size fluctuations – all of the traits projected strongly onto the two trait-scape axes. Instead, repeatable multitrait evolution occurs along a major axis of variation defined by several common diatom functional traits and the relationships among them. Because these functional traits are relevant to other phytoplankton functional groups ([30]), we expect the concept, utility, and many of the relationships revealed in any given phytoplankton trait-scape to generalize to other phytoplankton, especially within functional groups (silicifyers, calcifyers). This is because all phytoplankton have similar functional traits, and many these are linked to basic, conserved metabolism ([31]). However, we do not expect that all functional groups have exactly the same trait-scape, as functional groups with different biogeochemical functions could have different trait axes.

Our study used two environments, both of which were nutrient replete and below the temperature optimum for these strains. . While a similar degree of warming has been shown to drive adaptation in large laboratory populations of diatoms ([32,33]), major shifts in fundamental growth strategies, such as those associated with heat stress or nutrient starvation, would not be expected. If more extreme or stressful environments were included, it is possible that the ancestral trait-scape would not be suitable for describing evolved populations, especially if traits that do not vary in the ancestral environment become important for explaining variation between populations in the new environment. While our FSH populations did not experience heat stress, an increase of 4°C is in line with the magnitude of environmental change expected in many marine systems over the next 100 years ([34]). This is also the magnitude of change that a phytoplankton population might experience due to mixing between adjacent water masses ([35]), or growing sequentially over several seasons ([36]).

While individual traits did change in response to warming, multitrait phenotypes often returned to the ancestral location in the trait-scape. Based on this, we hypothesize that relative to individual trait values, multitrait phenotypes may be more stable across environmental gradients that do not provoke major shifts in growth strategies. Thus, trait-

scapes can offer insight into fundamental constraints on functional trait variation within phytoplankton groups. However, the stability of the trait-scape in the face of novel or stressful environments is unknown, and should be explored in future studies

The growth strategies of marine microbes coupled with their dynamic ocean habitats point to frequent bottlenecking in natural populations. While a low proportion of bottlenecked populations evolved new multitrait phenotypes, when this happens repeatedly over many populations, as will be the case in the ocean, population bottlenecks could generate substantial diversity in diatom functional traits and their correlations. This is consistent with bottlenecks generating diversity in other taxa that experience large fluctuations in population size, such as viruses and bacteria ([37,38]).

Population bottlenecks may be common in the natural environment, but they can also occur intentionally and unintentionally in laboratories. Specifically, laboratory practices associated with high mortality rates such as cryopreservation, antibiotic treatments, shipping cultures between locations and starting experiments from single cells, all result in bottlenecks. Our study demonstrates that population bottlenecks can cause changes in trait values and trait correlations, although this is relatively rare. Laboratory practices that involve one or more bottleneck events may explain some discrepancies between experiments with common or reference strains.

## Conclusions

Phytoplankton play crucial roles in aquatic food webs and biogeochemical cycling, and they do so through their interconnected web of functional traits. We show that higher order correlations among functional traits matter for revealing patterns of functional trait variation in phytoplankton. The trait-scape described by functional trait values and correlations in our study is robust to the variation that natural selection can produce in the short term, and across two similar and non-stressful environments. Most populations return to their ancestral locations in the trait-scape after demographic perturbations. However, a minority of populations do evolve different multitrait phenotypes from their own ancestors. These new phenotypes can be captured by movement on the trait-scape defined by the ancestral populations, often moving to areas of the trait scape that are already occupied (connecting peaks). Trait-scapes offer an alternative to master-trait based views of how trait correlations constrain multitrait phenotypes in diatoms, and we suggest that this same approach will also be useful in other phytoplankton functional groups. This multi-trait framework incorporates higher-level trait relationships and is a tractable way to understand and represent trait-based variation in phytoplankton.

## Materials and Methods

### Diatom cultures

Six strains of *Thalassiosira sp.* from the National Centre for Marine Algae and Microbiota at Bigelow were used: CCMP 1010, 1050, 1059, 1587, 2929 and 3367 (Table S1). These differed from each other in original isolation location, as well as traits such as cell size and population growth rate (see ref. [20] for a detailed description of the strains). Strains were chosen that did not clump or form chains in our culture conditions to allow easy isolation of a few cells for bottleneck transfers. Data from previous experiments using 13 different *Thalassiosira* strains including these six, confirmed that the strains used in this study are a representative divergent sample of a larger collection of genotypes ([20]).

### Culture maintenance

Cultures were grown in sterile f/2 media ([39]) made from natural sea water (collected in St Abbs, United Kingdom), at 20°C and approximately 60 µmol photons $m^{-2}$ $s^{-1}$ (measured with

a 4-pi sensor) at a 12h:12h light:dark cycle. Cultures were maintained in transparent 48-well plates covered with Breath-Easy breathable plate-seals (Sigma Aldrich). These culture conditions represent the control conditions.

**Evolution experiment**

The experiment was divided into two phases, an initial 3-month long reduced-selection (RS) phase (corresponding to 70-200 generations) followed by an 8-month full selection (FS) phase (200-500 generations) (Fig. 5).

The reduced-selection phase of the experiment was initiated with six replicates of each of the six experimental strains, resulting in a total of 36 experimental populations. Due to the extinction of three populations within the reduced-selection phase, 33 populations entered the full selection phase of the experiment. The full selection was performed in a control (FSC, 20°C) and a warm environment (FSH, 24°C). The warmed environment is below Topt for these strains and is not an obviously stressful growth environment.

Trait measurements of populations were performed at the beginning of the experiment, at the end of the reduced-selection phase and at the end of the full selection phase. During the experiment trait values were measured under control conditions, at the end of the experiment, trait values were obtained under control (20°C) and high temperature (24°C) assay conditions. Table S2 lists which traits values were collected for each experimental stage. Analyses have a focus on the data collected under control conditions. Whenever data from high temperature assay conditions is analysed, this is stated.

<u>Reduced-selection phase</u>

To reduce the efficacy of natural selection and allow divergent lower-fitness phenotypes to evolve, we repeatedly induced population bottlenecks (~8 cells) in the 36 experimental populations (six replicates of six ancestral strains). Initially, bottlenecks were induced every 7 days (corresponding to an average of 13 generations). As growth rates decreased over time, this time window was increased to every 14 days towards the end of the experiment (corresponding to an average of 18 generations). For laboratory feasibility, all populations were bottlenecked at the same time, as long as they had reached a minimum cell concentration of 2000 cells/mL. If cell concentrations were lower than 2000 cells/mL, cultures were diluted to 500 cells/mL instead, to allow for population recovery before a new bottleneck was induced.

The bottlenecking was performed in two dilution steps. First the most recent inoculation of each population was diluted to 2000 cells/mL. From this dilution the actual bottlenecking was performed aimed to transfer ~8 cells into 1 mL fresh media.

The bottlenecking was repeated 5-9 times, depending on the lineage. This corresponds to a total experiment length of 3 months and 70-200 generations, depending on population growth rates. Especially towards the end of the bottlenecking phase, single populations had decreased in growth to such a degree that they did not grow. In these cases the previous transfer was used to induce a new bottleneck. Throughout the reduced-selection phase the maximum growth rate was monitored via *in-vivo* fluorescence. At the end of the bottleneck phase, population growth rates were reduced by an average of 45% compared to ancestral growth rates (Fig. S3).

<u>Full selection phase</u>

During the subsequent full selection phase populations were propagated by batch culture with transfer sizes of ~1000 cells every 7 days. 33 populations entered this phase. The full selection was performed in two environments, a control (20°C) and a warm environment (24°C) to allow for the later comparison of plastic and evolutionary responses to different conditions. The warm environment was chosen to create a selection regime that clearly diverges from the control environment without stressing the weakened reduced-selection populations to such a degree that they would die (based on the provided information on temperature ranges for the ancestral populations by the Bigelow culture collection). As an example, from the ancestral strain 1010, 6 replicates underwent the reduced selection (called 1010-1 to 1010-6), in the full selection phase each replicate was exposed to two temperature

environments (named 1010-1C to 1010-6C and 1010-1H to 1010-6H). In total, populations were transferred ~25 times in the full selection phase of the experiment, corresponding to 200-500 generations. Maximum growth rates were measured every 5 to 10 transfers throughout the full selection phase to monitor fitness recovery. Before the final trait measurements the growth rate of all populations was measured over four transfers (four weeks) to ensure that the population growth rates had stabilized, indicating that populations were on or near a local high-fitness solution (Fig. S4, S5).

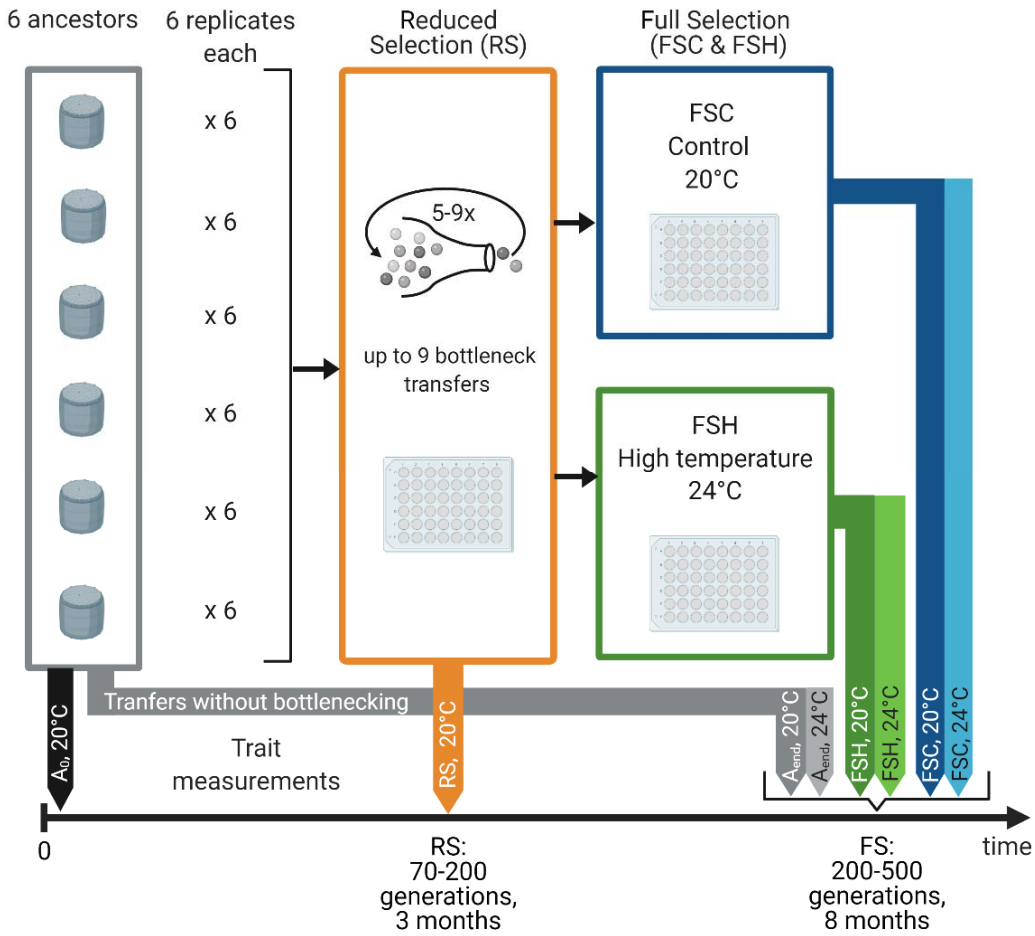


**Figure 5.** Schematic of the experimental design. Six strains (1010, 1050, 1587, 2929, and 3367) were used for the experiment. Six replicates from each strain (1010-1, -2, ..-6, 1050-1,…) underwent a procedure of up to 9 bottlenecks, each time transferring ~8 cells. After that, lineages were transferred regularly for 8 months under full selection with large inoculation sizes. The full selection was performed under control (1010-1C, 1010-2C,…) and high temperature conditions (1010-1H, 1010-2H,…). Phenotypic trait measurements under control assay conditions took place at the beginning of the experiment (from the ancestral strains, $A_0$), and at the end of the reduced selection phase (RS). At the end of the full selection phase, trait measurements of all ancestral ($A_{end}$), evolved control (FSC) and high temperature lineages (FSH) were performed under control and high temperature assay conditions.

### Trait measurements

To investigate how trait values changed throughout the experiment, trait measurements were performed at the onset of the experiment (A0), at the end of the reduced-selection phase (RS) and at the end of the full selection phase (FSC, FSH). At the end of the full selection phase, the experimental ancestors, which were maintained under control conditions throughout the experiment, were measured again to account for any trait change during normal culture maintenance (Aend). Where applicable, all traits were measured during mid-

exponential growth phase and daily mid-light phase. A detailed illustration of single trait changes across the experiment can be found in Fig. S7.
Trait measurements at the beginning and at the end of the reduced-selection phase included maximum growth rate, cell size, cell complexity, chlorophyll a content, and particulate organic carbon and nitrogen content. At the end of the full selection phase, a more extensive set of traits were measured for the FSC- and FSH-populations and the experimental ancestors, in both the control and the hot environment, Table S2. Pilot data showed that populations reach stable trait values after acclimating for 7 days to the test environment ([20,24]).Therefore, trait measurements were performed for all populations after an acclimation period of 7 days (one transfer) in the test environment. All trait measurements are described below.

Growth rate

Growth rates were measured via daily *in-vivo* fluorescence using a plate reader (excitation: 455nm, emission: 620nm; Tecan Spark, United Kingdom). The exponential growth rate was calculated for each time step using:

$$\mu = \frac{\ln(x_2) - \ln(x_1)}{t_2 - t_1} \qquad [1]$$

Maximum growth rates were determined based on the average growth over 4 consecutive time steps. During the bottleneck phase growth rates were determined based on single replicates per evolving population; for the final trait measurements growth rates of all ancestral and back-selected populations were determined based on 3 replicates per evolving population.

Cell size, cell complexity and chlorophyll a

Cell size, cell complexity and chlorophyll a concentration of all populations were determined by flow cytometry. Cell size estimates were determined based on the median forward scatter area, and converted to µm using a standard curve based on standard beads of 1, 3, 6, 10 and 25 µm bead size. The resulting values for cell size corresponds to the cell diameter.

Cell complexity was estimated based on median side scatter area, chlorophyll a (Chl a) was determined based on median fluorescence in the PerCP-Cy5-5-A channel (488nm wavelength, filter 695/40BP).

Particulate organic carbon and nitrogen

Particulate organic carbon (POC) and nitrogen (PON) content were determined using elemental analysis. Populations were grown in 50 mL culture flasks containing 45 mL of media, up to a cell density of ~112,000 cells/mL. The culture was split into two technical replicates of 20 mL, which were applied onto pre-combusted Whatman GFF filters. From the remaining sample volume cell concentrations were determined using *in-vivo* fluorescence and previously determined fluorescence standard curves for each strain. The dry weight of the cells was determined after drying the filters over 2 days at 40°C. Filters were then treated to remove potential dissolved organic carbon. To do so, the filters were dampened with 200 µL distilled water, and 100 µL 2M hydrochloric acid was then applied to remove any inorganic carbon. After air-drying filters overnight, the samples were analyzed in a Thermo Fisher Scientific FlashSMART 2000 Elemental Analyzer.

Lipid content, silicic acid uptake and production of reactive oxygen species

The neutral lipid content, silicic acid uptake and production of reactive oxygen species were determined based on ([24]). In summary, neutral lipid content of cells was determined by adding a BODIPY 505/515 stain to the samples, at a final concentration of 2.6 µg/mL of BODIPY. After 10 min incubation, samples were analysed in the flow cytometer using median FITC-A (488nm wavelength, filter 530/30 BP).

Silicic acid uptake was calculated from PDMPO uptake by inoculating 500 µL samples with 0.125 µmol/L PDMPO dye (LysoSensor™ Yellow/Blue DND-160, Invitrogen) for 24 h, blank samples were inoculated in the same way excluding the dye. PDMPO is incorporated by cells with the same rate as silicic acid, allowing an estimate of the rate of silica production. After incubation under 12h:12h light:dark conditions silicic acid uptake was determined using median AmCyan-A of the flow cytometer, subtracting values of undyed samples from the dyed samples.

Relative intracellular ROS as a measure of stress was determined using H2DCFDA dye. 500 µL sample volumes were inoculated for 5 hours in the dark in the test environment (20/24°C) with a concentration of 80 µmol/L dye. Blank population samples excluding dye were inoculated in the same manner. After incubation relative intracellular ROS was calculated from H2DCFDA fluorescence using a Tecan Spark plate reader (excitation: 488nm, emission: 525nm) and blank values were subtracted from the dyed samples values.

**Data analysis**

Data were analysed and plotted using Matlab, statistical analyses were performed in the R environment.

Correction for influence of cell size on other traits

Cell size is known to be a major functional trait, influencing many other functional traits; many metabolic traits show a linear correlation with cell size ([40]). We corrected the analyses of correlation matrices and principal components by the influence of cell volume. Traits that were corrected for cell volume were granularity, Chl a, lipid content, ROS production, silicic acid uptake, POC content and PON content. Growth rate and POC/PON ratio were not corrected for cell volume, since there is no linear relationship between growth rate and cell size ([40]) and since the ratio between POC and PON should not necessarily be correlated with cell size. The cell volume correction was performed by dividing the trait value of each sample by the corresponding calculated cell volume. Cell volume was calculated based cell diameter, assuming a spherical shape.

$$Sample\ trait\ value_{corrected} = \frac{Sample\ trait\ value_{original}}{\frac{4}{3} \times \pi \times \left(\frac{cell\ diameter[\mu m]}{2}\right)^3} \qquad [2]$$

Principal component analysis

Principal component analyses (PCA) were performed after standardizing all trait data. The number of traits that were included in individual analyses differed slightly from each other, since not all traits were measured in all environments for all experimental stages (Table S2). To project other populations into a defined PCA space, their normalized trait values are multiplied by the coefficients of the PCA space.

Analysis of trait-scape connectivity

To analyse the connectivity of the trait-scape, high-fitness (ancestral, FSC and FSH) locations were categorized as isolated, connected or novel. To maximize the comparability between analyses, this analysis was performed based on the PCA including trait values of ancestral and full selection populations under control assay conditions. Trait values of reduced selection populations were projected into the trait-scape.

First, populations that returned to the ancestral peak were identified by calculating the Euclidean distance between ancestral peak and location after reduced selection, and the distance between ancestral peak and location after full selection. If the latter distance was smaller than the former, the peak of the full selection population was classified as an isolated fitness peak.

For all already classified isolated fitness peaks, a 75% confidence interval was calculated around the ancestral peak. All populations that did not meet the first criterion, but remained in this 75% confidence interval of their ancestor were also classified as isolated fitness peaks.

Any population, that was not classified as an isolated fitness peak and that moved into the 75% confidence interval of another strain, was classified as a connected fitness peak.
All remaining populations that were neither classified as having an isolated peak nor a connected fitness peak, were considered to have found a previously unoccupied location in trait-scape, referred to as novel fitness peak.

Outlier analysis

To identify outliers among the FSC and FSH populations that diverged from ancestral trait values and trait correlations, all possible pairwise trait correlations were calculated for ancestors, FSC and FSH populations under control conditions. Across all ancestral strains linear regressions with a 95% confidence interval were calculated (Fig. S8). The residual values for FSC and FSH populations that diverged from the ancestral 95% confidence were calculated, all residual values for trait correlations that stayed within the ancestral confidence interval were set to zero. For each population an outlier score was calculated as the mean residual value across all pairwise trait correlations.

Statistical analysis

To compare the intra-vs. interspecific variation in trait-scape, Euclidean distances between all ancestral, FSC and FSH populations were calculated based on their location in the trait-scape using Matlab. The resulting dataset was classified by strain and grouped into intraspecific or interspecific Euclidean distances. Statistical analysis was then performed in the R environment using the nlme and lme4 packages. Since both a visual check via Q-Q plot and the Levene test suggested that the data is not normally distributed, a generalized linear mixed-effects model was applied with type of variation (inter- vs. intraspecific) as fixed effect and strain as random effect.

## Acknowledgments

The authors would like to thank Toby Samuels, Carmen Robinson and Katy McDonald for their help with lab work. Flow cytometry data were generated within the Flow Cytometry and Cell Sorting Facility in Ashworth, King's Buildings at the University of Edinburgh. The authors thank Martin Waterfall for his support with flow cytometry analyses. Particulate organic carbon and nitrogen analyses were performed by the Chemical Analysis Facilities of the School of Geosciences at the University of Edinburgh. The authors thank Gavin Sim and Joe Casillo for their help with elemental analyses. This research was supported by the Gordon and Betty Moore Foundation Marine Microbes Initiative (MMI 7397 to MD, NML and SC). For the purpose of open access, the author has applied a Creative Commons Attribution (CC BY) licence to any Author Accepted Manuscript version arising from this submission.

## References

1. Ward, B. A., Cael, B., Collins, S. & Young, C. R. Selective constraints on global plankton dispersal. *Proc Natl Acad Sci USA* **118**, (2021).
2. Wolf, K. K. *et al.* Company matters: The presence of other genotypes alters traits and intraspecific selection in an Arctic diatom under climate change. *Glob. Change Biol.* **25**, 2869–2884 (2019).
3. Sjöqvist, C. Evolution of Phytoplankton as Estimated from Genetic Diversity. *J Mar Sci Eng* **10**, 456 (2022).
4. Franks, S. J., Hoffmann, A. A., & others. Genetics of climate change adaptation. *Annu Rev Genet* **46**, 185–208 (2012).
5. Brennan, G. L., Colegrave, N. & Collins, S. Evolutionary consequences of multidriver environmental change in an aquatic primary producer. *Proc Natl Acad Sci USA* **114**, 9930–9935 (2017).
6. Doblin, M. A. & Van Sebille, E. Drift in ocean currents impacts intergenerational microbial exposure to temperature. *Proc Natl Acad Sci USA* **113**, 5700–5705 (2016).
7. Jönsson, B. F. & Watson, J. R. The timescales of global surface-ocean connectivity. *Nat Commun* **7**, 1–6 (2016).
8. Walworth, N. G., Zakem, E. J., Dunne, J. P., Collins, S. & Levine, N. M. Microbial evolutionary strategies in a dynamic ocean. *Proc Natl Acad Sci USA* **117**, 5943–5948 (2020).
9. Wielgoss, S. When maths meets phytoplankton ecology. *Nat Ecol Evol* **6**, 138–139 (2022).

10. Rengefors, K., Kremp, A., Reusch, T. B. & Wood, A. M. Genetic diversity and evolution in eukaryotic phytoplankton: revelations from population genetic studies. *J Plankton Res* **39**, 165–179 (2017).
11. Clayton, S., Dutkiewicz, S., Jahn, O. & Follows, M. J. Dispersal, eddies, and the diversity of marine phytoplankton. *Limnol Ocean.* **3**, 182–197 (2013).
12. Sassenhagen, I., Sefbom, J., Säll, T., Godhe, A. & Rengefors, K. Freshwater protists do not go with the flow: population structure in G onyostomum semen independent of connectivity among lakes. *Env. Microbiol* **17**, 5063–5072 (2015).
13. Godhe, A. & Härnström, K. Linking the planktonic and benthic habitat: genetic structure of the marine diatom Skeletonema marinoi. *Mol Ecol* **19**, 4478–4490 (2010).
14. Chen, Z. *et al.* Prochlorococcus have low global mutation rate and small effective population size. *Nat. Ecol. Evol.* **6**, 183–194 (2022).
15. Sefbom, J., Sassenhagen, I., Rengefors, K. & Godhe, A. Priority effects in a planktonic bloom-forming marine diatom. *Biol Lett* **11**, 20150184 (2015).
16. Ward, B. A., Dutkiewicz, S., Jahn, O. & Follows, M. J. A size-structured food-web model for the global ocean. *Limnol Ocean.* **57**, 1877–1891 (2012).
17. Dutkiewicz, S. *et al.* Dimensions of marine phytoplankton diversity. *Biogeosciences* **17**, 609–634 (2020).
18. Litchman, E. Trait-Based Diatom Ecology. in *The Molecular Life of Diatoms* 3–27 (Springer, 2022).
19. Lindemann, C., Fiksen, Ø., Andersen, K. H. & Aksnes, D. L. Scaling laws in phytoplankton nutrient uptake affinity. *Front Mar Sci* **3**, 26 (2016).
20. Argyle, P. A. *et al.* Multivariate trait analysis reveals diatom plasticity constrained to a reduced set of biological axes. *ISME Comm* **1**, 1–11 (2021).
21. Malcom, J. W. *et al.* Extensive cross-environment fitness variation lies along few axes of genetic variation in the model alga, C hlamydomonas reinhardtii. *New Phytol.* **205**, 841–851 (2015).
22. Walworth, N. G. *et al.* The evolution of trait correlations constrains phenotypic adaptation to high CO2 in a eukaryotic alga. *Proc. R. Soc. B Biol. Sci.* **288**, 20210940 (2021).
23. Lenski, R. E. *et al.* Sustained fitness gains and variability in fitness trajectories in the long-term evolution experiment with Escherichia coli. *Proc R Soc B Biol Sci* **282**, 20152292 (2015).
24. Argyle, P. A. *et al.* A High-Throughput Assay for Quantifying Phenotypic Traits of Microalgae. *Front Microbiol* 2910 (2021).
25. Jin, P. & Agustí, S. Fast adaptation of tropical diatoms to increased warming with trade-offs. *Sci. Rep.* **8**, 1–10 (2018).
26. Schaum, C.-E. Enhanced biofilm formation aids adaptation to extreme warming and environmental instability in the diatom Thalassiosira pseudonana and its associated bacteria. *Limnol Ocean.* **64**, 441–460 (2019).
27. Malerba, M. E. & Marshall, D. J. Testing the drivers of the temperature–size covariance using artificial selection. *Evolution* **74**, 169–178 (2020).
28. Carrara, F., Sengupta, A., Behrendt, L., Vardi, A. & Stocker, R. Bistability in oxidative stress response determines the migration behavior of phytoplankton in turbulence. *Proc Natl Acad Sci USA* **118**, e2005944118 (2021).
29. D'Autréaux, B. & Toledano, M. B. ROS as signalling molecules: mechanisms that generate specificity in ROS homeostasis. *Nat Rev Mol Cell Biol* **8**, 813–824 (2007).
30. Litchman, E. *et al.* Global biogeochemical impacts of phytoplankton: a trait-based perspective. *J Ecol* **103**, 1384–1396 (2015).
31. Kremer, C. T., Thomas, M. K. & Litchman, E. Temperature-and size-scaling of phytoplankton population growth rates: Reconciling the Eppley curve and the metabolic theory of ecology. *Limnol. Oceanogr.* **62**, 1658–1670 (2017).
32. O'Donnell, D. R. *et al.* Rapid thermal adaptation in a marine diatom reveals constraints and trade-offs. *Glob Change Biol* **24**, 4554–4565 (2018).
33. Listmann, L., LeRoch, M., Schlüter, L., Thomas, M. K. & Reusch, T. B. Swift thermal reaction norm evolution in a key marine phytoplankton species. *Evol Appl* **9**, 1156–1164 (2016).
34. Masson-Delmotte, V. *et al.* IPCC Climate change 2021: the Physical Science Basis. *Contrib. Work. Group Sixth Assess. Rep. Intergov. Panel Clim. Change* 2 (2021).
35. Zaiss, J., Boyd, P. W., Doney, S. C., Havenhand, J. N. & Levine, N. M. Impact of Lagrangian Sea Surface Temperature Variability on Southern Ocean Phytoplankton Community Growth Rates. *Glob. Biogeochem Cycles* **35**, e2020GB006880 (2021).
36. Ralston, D. K., Keafer, B. A., Brosnahan, M. L. & Anderson, D. M. Temperature dependence of an estuarine harmful algal bloom: Resolving interannual variability in bloom dynamics using a degree-day approach. *Limnol Ocean.* **59**, 1112–1126 (2014).
37. Windels, E. M. *et al.* Population bottlenecks strongly affect the evolutionary dynamics of antibiotic persistence. *Mol Biol Evol* **38**, 3345–3357 (2021).
38. Bull, R. A. *et al.* Sequential bottlenecks drive viral evolution in early acute hepatitis C virus infection. *PLoS Pathog* **7**, e1002243 (2011).
39. Guillard, R. R. Culture of phytoplankton for feeding marine invertebrates. in *Culture of Marine Invertebrate Animals* 29–60 (Springer, 1975).
40. Marañón, E. Cell size as a key determinant of phytoplankton metabolism and community structure. *Annu. Rev. Mar. Sci.* 241–264 (2015).